Development 130, 3283-3295
© 2003 The Company of Biologists Ltd
doi:10.1242/dev.00542

Mutations in *Arabidopsis* condensin genes disrupt embryogenesis, meristem organization and segregation of homologous chromosomes during meiosis

Najeeb U. Siddiqui, Patricia E. Stronghill, Ronald E. Dengler, Clare A. Hasenkampf and C. Daniel Riggs*

Department of Botany, Division of Life Sciences, University of Toronto, 1265 Military Trail, West Hill, Ontario M1C 1A4, Canada
*Author for correspondence (e-mail: riggs@utsc.utoronto.ca)

Accepted 10 April 2003

SUMMARY

Proper chromatin condensation and sister chromatid resolution are essential for the maintenance of chromosomal integrity during cell division, and is in part mediated by a conserved multisubunit apparatus termed the condensin complex. The core subunits of the complex are members of the SMC2 (Structural Maintenance of Chromosomes) and SMC4 gene families. We have cloned an *Arabidopsis* gene, *AtCAP-E1*, which is a functional ortholog of the yeast *SMC2* gene. A second, highly homologous SMC2 gene, *AtCAPE-2*, was identified by the *Arabidopsis* genome project. SMC2 gene expression in *Arabidopsis* was correlated with the mitotic activity of tissues, with high level expression observed in meristematic cells. The two genes are differentially expressed with *AtCAP-E1* accounting for more than 85% of the total SMC2 transcript pool. The *titan3* mutant is the result of a T-DNA insertion into *AtCAP-E1*, but other than subtle endosperm defects, *titan3* is viable and fecund. We identified a T-DNA insertion mutant of *AtCAP-E2*, which showed no obvious mutant phenotype, indicating that the two genes are functionally redundant. Genetic crosses were employed to examine the consequences of reduced SMC2 levels. Both male and female gametogenesis were compromised in double mutant spores. Embryo lethality was observed for both double homozygous and *AtCAP-E1*$^{-/-}$, *AtCAP-E2*$^{+/-}$ plants; arrest occurred at or before the globular stage and was associated with altered planes of cell division in both the suspensor and the embryo. Down regulation of both genes by antisense technology, as well as in *AtCAP-E1*$^{+/-}$, *AtCAP-E2*$^{-/-}$ plants results in meristem disorganization and fasciation. Our data are consistent with the interpretation that threshold levels of SMC2 proteins are required for normal development and that AtCAP-E2 may have a higher affinity for its target than AtCAP-E1.

Key words: Condensation, Meristem, Meiosis, Fasciation, *Arabidopsis thaliana*, SMC2, Gametogenesis

INTRODUCTION

Chromatin condensation is a fundamental cellular process in which entangled interphase chromatin fibers are actively resolved and packaged into physically discrete and compact chromosomes that undergo segregation during cell division. This complex series of events enables the cell to proceed through mitosis and faithfully distribute genetic information to each daughter cell. The inability to execute this process correctly can result in catastrophic chromosome segregation defects as is observed in mutants defective in topoisomerase II (DiNardo et al., 1984). Failure to disentangle chromatin fibers prevents compaction necessary for mitotic chromosome condensation (Gimenez-Abian et al., 2000; Cuvier and Hirano, 2003). In addition to topoisomerase II, other conserved proteins and histone modifications play roles in chromosome condensation (Hirano, 2002).

The SMC proteins are evolutionarily conserved across phylogenetic kingdoms with representatives in both prokaryotes and eukaryotes. The eukaryotic SMC proteins can be subdivided into six distinct subfamilies (SMC1-6) (Hirano, 2002; Jessberger, 2002), and three functional categories can be defined based on the formation of their heterodimers. The SMC2/SMC4 heterodimers assemble with three other non-SMC proteins to form the 'condensin' complex, which is involved in mitotic chromosome condensation and dosage compensation (Hirano and Mitchison, 1994; Lieb et al., 1998; Sutani et al., 1999; Kimura et al., 2001). Members of the SMC1 and SMC3 families form heterodimers to give rise to the 'cohesin' complex, which is involved in sister chromatid cohesion (Michaelis et al., 1997; Losada et al., 1998). Lastly, SMC5 and SMC6 members form heterodimers that are involved in DNA recombination/repair (Mengiste et al., 1999; Fousteri and Lehmann, 2000). All SMC proteins consist of five distinct domains: nucleotide-binding domains located at the N and C termini lie adjacent to two coiled-coil regions, which are separated by a hinge region (Hirano, 2002; Jessberger, 2002). The catalytic function of the SMC subunits is regulated by non-SMC members of these multisubunit complexes. Mutations in genes encoding components of SMC complexes result in a variety of defects, ranging from lethality to developmental abnormalities (Saka et al., 1994; Strunnikov et al., 1995; Bhat et al., 1996; Lieb et al., 1998; Freeman et al., 2000; Steffensen et al., 2001; Bhalla et al., 2002; Hagstrom et al., 2002).

In both plants and animals, alterations in chromatin structure and dynamics are implicated as factors controlling both cell cycle progression and aspects of development (reviewed by Muller and Leutz, 2001; Reyes et al., 2002; Berger and Gaudin, 2003). Whereas in many metazoans mutations in these genes are lethal, orthologous mutants in plants are often tolerated, resulting in developmental and/or physiological defects (Wagner, 2003). For example, plants harboring an antisense construct of histone deacetylase 1 (*AtHD1*) exhibit pleiotropic defects in growth and development, and some of these could be correlated with ectopic expression of the *SUPERMAN* gene (Tian and Chen, 2001). Similarly, disruption of the topoisomerase I gene leads to phyllotaxy defects and bifurcation of lateral shoots (Takahashi et al., 2002). *Arabidopsis* plants deficient in telomerase function also exhibit developmental abnormalities with grossly enlarged meristems, altered leaf morphology and low viable seed set (Riha et al., 2001). Lastly, mutations in chromatin assembly factor (CAF1) subunits, which assemble nucleosomes onto nascent DNA, underpin the *fasciata* phenotype (Kaya et al., 2001).

Despite significant progress in our understanding of molecular and biochemical aspects of chromatin remodeling and chromosome condensation in yeast and in animal systems, very little information exists in plants. *Arabidopsis* affords an excellent system to explore these basic cellular processes as the genome has been sequenced and annotated, genetic manipulations are facile, and there exists a large collection of insertion mutant lines for reverse genetics studies. We therefore sought to identify mutations in *Arabidopsis* condensin genes. Here we report the characterization of two *Arabidopsis* SMC2 genes, *AtCAP-E1* and *AtCAP-E2* (*Arabidopsis thaliana* Chromosome Associated Protein subunit E, a nomenclature that conforms to the designation given to SMC2 orthologs in higher eukaryotes). Unlike other characterized diploid organisms, *Arabidopsis* contains two members of the SMC2 family. Recently, a T-DNA insertion into *AtCAP-E1* was reported to be responsible for the *titan3* mutant, which exhibits enlarged endosperm nuclei and aberrant mitotic figures but otherwise develops normally and is fecund (Liu et al., 2002). Given the essential role for SMC2 proteins in chromosome condensation in other organisms, it could be predicted that disruption of SMC2 function would have profound effects on cell division and plant development. We identified a mutant of *AtCAP-E2*, which exhibits no obvious developmental defects, but the *AtCAP-E1*$^{-/-}$, *AtCAP-E2*$^{-/-}$ double mutant results in embryo lethality. Transgenic plants expressing an antisense construct exhibited reduced levels of both SMC2 transcripts, and pleiotropic phenotypes including slow growth, disorganized meristems, and fasciation. Our data indicate that proper developmental patterning requires a threshold level of SMC2 proteins to support condensin complex function.

MATERIALS AND METHODS

Identification and cloning of the *Arabidopsis* SMC2 gene *AtCAP-E1*

Based on the conserved amino acid sequences, FNAITGLN and PHFLIMQG, which flank the NTP-binding domain of SMC2 proteins, degenerate oligonucleotide primers (5′CCYTGCATRATIARR-AARTKWGG3′ and 5′TTYAAYGCIATYACIGGWYTIAAYGG3′) were designed to PCR amplify *Arabidopsis* genomic DNA. The PCR fragment was used to screen an *Arabidopsis* genomic library by standard methods, and a lambda genomic clone was isolated. The *AtCAP-E1* cDNA was isolated by RT-PCR. A primer corresponding to the last eight amino acids and the stop codon of *AtCAP-E1* (5′-TCACTTGGTCTGCTTTG TTACTGTCC-3′) was used for RT with 1 μg of total RNA from young seedlings. PCR was performed using the primer employed for RT and a forward primer (5′-ATGCATATAAAG-GAGATATGCTTGG-3′) encoding the first eight amino acids of the *AtCAP-E1* protein. The sequence of the 3528 bp cDNA has been deposited in the GenBank database under accession number AF306547.

Yeast complementation

The *AtCAP-E1* cDNA was digested with *Not*I and *Spe*I and ligated into the *Not*I and *Xba*I sites in pYES2. Transformation of *smc2-Δ6* cells was performed according to the method of Gietz and Woods (Gietz and Woods, 1998). Transformants were selected at the restrictive temperature (37°C) on DOB dropout base plus CSM lacking uracil containing 2% D-galactose. For 4′,6-diamidino-2-phenylindole (DAPI) staining, liquid cultures [wild type (YPH499), *smc2-Δ6*, and transformed cells] were grown overnight at 30°C and then shifted to 37°C for 2 hours. An aliquot of cells was harvested, fixed in 2.5% glutaraldehyde, rinsed, and stained with 2 μg/ml DAPI solution. DAPI staining was monitored using a Zeiss axiophot microscope.

RNA isolation and RT-PCR analysis

Total RNA was prepared from *Arabidopsis* roots, stems, mature leaves, floral buds and mature green siliques using the TRIZOL (Gibco) reagent. RT-PCR was performed as follows. Forward (5′-GATACATGCAAAGATGAAGGAATG-3′) and reverse (5′-TAT-CATTCTTCCTATGTTCTGTGTGTG-3′) primers were used to amplify a 762 bp fragment from both *AtCAP-E1* and *AtCAP-E2*. First-strand cDNA synthesis was performed with 1 μg of total RNA and the backward primer in a 25 μl reaction according to the 5′RACE protocol (Gibco). PCR was performed by making tenfold serial dilutions (10^{-1} and 10^{-2}) starting from the same amount of first-strand cDNA. The volume of each tenfold RT-dilution step used as a template was 6% of the final PCR volume. For CAPS analysis (Konieczny and Ausubel, 1993), PCR products were digested with *Ssp*I or *Xba*I and DNA gel blotting was performed with the 762 bp cDNA fragment as the probe.

Construction of *AtCAP-E1* promoter::β-glucuronidase gene and plant transformation

A 2.7 kb region upstream of the *AtCAP-E1* start codon was amplified by PCR with the primers: 5′-CGGGATCCAGCAATAGCTTTAGCT-TTCGCC-3′ and 5′-TCCCCCGGGCTTCCTTCTTCTTCTTCCCC-3′. The amplified fragment was ligated into pBI101.2 (Jefferson et al., 1987) upstream of the β-glucuronidase gene. The construct was mobilized into *Agrobacterium* (GV3101) and used to transform (Landsberg *erecta* ecotype) plants by the floral dip method (Clough and Bent, 1998). Transformants were selected on Murashige and Skoog (MS) plates (1× MS salts pH 5.7, 3% sucrose, 0.5 g/l MES, 0.8% phytagar) containing 50 μg/ml kanamycin. The histochemical assay for GUS was performed as described previously (Jefferson et al., 1987).

In situ hybridization

In situ hybridization was performed essentially as described by Jackson (Jackson, 1991). A 196 bp region of the *Arabidopsis* histone H4 gene was labeled with digoxigenin. In vitro transcription was performed following the manufacturer's (Roche) protocol. Wild-type and antisense seedlings were fixed in FAA (3.7% formaldehyde, 5% acetic acid, 50% ethanol) for 2 hours, dehydrated in an ethanol/Histoclear series, embedded in TissuePrep and sectioned at

10 μm. After the color development, sections were mounted in VectaShield mounting medium (Vector Laboratories, USA) and photographed using a Zeiss axiophot microscope and digital imaging system.

Isolation of an *AtCAP-E2*$^{-/-}$ mutant

A BLAST search in the SAIL (Syngenta Arabidopsis Insertion Library) database with the *AtCAP-E2* genomic sequence (AGI identifier At3g47460) revealed a line (36-C09) with a T-DNA insertion near the 3′ end of the gene. Seeds of this line were germinated on MS plates containing glufosinate ammonium (BASTA) to select for plants having a T-DNA insertion. The integration site of the T-DNA was determined by PCR amplification and sequencing of a 1061 bp fragment using a gene-specific primer (5′ GATACATG-CAAAGATGAGGAATG-3′) and the T-DNA left border primer (5′-TAGCATCTGAATTTCATAACCAATCTCGATACAC-3′). The genotype of the individual plants grown on BASTA was determined by two sets of PCR reactions. The first used gene-specific primers flanking the T-DNA (5′-GATACATGCAAAGATGAAGGAATG-3′; 5′-TATCATTCTTCCTATGTTCTGTGTGTG-3′) to identify the presence of a wild-type allele. Plants heterozygous for the T-DNA insertion gave rise to a 1491 bp *AtCAP-E2* gene fragment with PCR primers flanking the T-DNA insertion site, while no band corresponding to the *AtCAP-E2* locus was amplified from the homozygous plants. The second PCR employed a gene-specific primer and the T-DNA left border primer to confirm the presence of a mutant allele.

Generation of double mutants and analysis of F_2 progeny

Double mutant plants were generated by crossing homozygous *AtCAP-E1*$^{-/-}$ (*ttn3* mutant; Wassilewskija ecotype; WS) with *AtCAP-E2*$^{-/-}$ (Columbia ecotype; Col) plants. F_1 seeds were germinated on medium containing both BASTA and kanamycin and 100% resistance to both antibiotics was observed (The T-DNA insertion at the *AtCAP-E1* locus confers kanamycin resistance while the T-DNA insertion at the *AtCAP-E2* locus confers BASTA resistance). F_2 seedlings were selected on MS plates containing both antibiotics, and 180 F_2 seedlings were genotyped by employing three sets of primers. Based on the site of insertion of the T-DNAs, the first primer pair (5′-GATACATGCAAAGATGAAGGAATG-3′; 5′-TATCATTCTTCCT-ATGTTCTGTGTGTG-3′) was chosen to flank the insertion sites and amplification of 1.65 kb (amplified from the *AtCAP-E1* locus) and 1.49 kb (amplified from the *AtCAP-E2* locus) fragments are indicative of a wild-type allele. Amplification of a single band (either 1.65 or 1.49) represented heterozygosity at the given locus and homozygosity for a T-DNA insertion in the other gene. The other sets of primer pairs employed an allele-specific primer together with a T-DNA primer to test for the presence of a T-DNA insertion as described in the previous section.

Because the two single mutants are in different genetic backgrounds (WS and Col) we crossed these wild-type plants to determine if any inter-ecotype incompatibilities exist that would compromise development and/or fecundity. We observed no evidence of ovule or embryo abortion, which validates the phenotypic defects observed in the F_2 progeny of a cross between the single mutants. Genetic evidence supporting this contention is twofold. In siliques of E1$^{+/-}$, E2$^{+/-}$ plants, the number of aborted ovules and aborted embryos conformed to the ratios expected based on the parental genotype (data not shown) such as they did in E1$^{+/-}$, E2$^{-/-}$. Secondly, the anaphase bridges observed in *AtCAP-E1*$^{+/-}$, *AtCAP-E2*$^{-/-}$ pollen mother cells were not observed in *AtCAP-E1*$^{+/-}$, *AtCAP-E2*$^{+/-}$ pollen mother cells.

Generation of antisense transgenic plants

Arabidopsis plants (Landsberg *erecta* ecotype) carrying the *AtCAP-E1* cDNA in an antisense orientation were generated by inserting a 2.3 kb fragment of the *AtCAP-E1* cDNA in the reverse orientation in pBI121, such that transcription of the antisense strand was driven by the CaMV-35S constitutive promoter. Transgenic plants were generated as described above. All plants were grown at 25°C under a 16-hour light/8-hour dark regime.

Histological analysis

Siliques were dissected after fixation in an ethanol:acetic acid (3:1) solution, cleared overnight in chloral hydrate:glycerol:water (8:2:1) and imaged by Nomarski optics.

For DAPI staining of pollen mother cells, fresh anthers were dissected on a slide in 40 μl of 10 mM sodium citrate buffer pH 4.0 using a needle under a dissecting misroscope. After releasing the contents of the anthers the sample was mounted in 15 μl of Vectashield containing DAPI. After the addition of a coverslip, the slides were viewed by fluorescence using a Zeiss Axiophot microscope.

For Toluidine Blue and DAPI staining of SAMs, 8-day-old wild-type and 18-day-old antisense seedlings were fixed in FAA, embedded in wax, and 8 μm sections were cut. Images were captured with a Zeiss axiophot microscope equipped with a digital image capture system.

For scanning electron microscopy (SEM), seedlings were fixed in FAA, dehydrated, critical point dried, and coated with gold particles. Specimens were viewed using a Hitachi S-2500 microscope.

Wild-type and antisense seedlings were grown vertically on agar plates for 10 days for confocal laser scanning microscopy (CLSM). For Aniline Blue staining, roots were fixed in a 2.5% NaOH/0.1% sodium dodecyl sulfate solution for 18 hours at room temperature, rinsed in water, and dehydrated by passing through an ethanol series. The tissue was stained for 4 hours with 0.4% Aniline Blue. After staining, tissue was dehydrated to 100% ethanol and cleared by passing through a 3:1, 1:1 and 1:3 series of ethanol:methyl salicylate solution followed by two washes in 100% methyl salicylate. Median longitudinal optical sections of the root tip were obtained using an Olympus Fluoview (FV5-PSU) CLSM.

Immunoblotting

A 1302 bp *Dra*I to *Eco*RI fragment of the *AtCAP-E1* cDNA was cloned between *Sma*I and *Eco*RI sites of pGEX2TK (Invitrogen) vector downstream of the glutathione S-transferase (GST) fragment to produce a GST-tagged recombinant protein in bacteria. The recombinant protein was purified and used to immunize rabbits. The affinity-purified polyclonal antibodies were diluted 1:2500 for immunoblotting with total protein extracts prepared from 7-day-old seedlings.

RESULTS

Arabidopsis contains two SMC2 genes

Based on a sequence alignment of SMC2 proteins, we designed degenerate oligonucleotide primers to amplify an *Arabidopsis* genomic fragment encoding the conserved amino terminal nucleotide-binding domain. Sequencing of this fragment and computer analysis confirmed its identity as an SMC2 gene fragment located on chromosome V, and we used the fragment as a hybridization probe to screen a genomic library for the complete gene, which we termed *AtCAP-E1*. Based on the genomic sequence information we designed primers corresponding to the ends of the coding region of the gene and employed RT-PCR to amplify the cDNA. Comparison of cDNA and genomic sequences confirmed the intron/exon boundaries predicted by computer annotation. In parallel, the *Arabidopsis* Genome Initiative (AGI) reported the sequencing of a second SMC2 gene, which resides on chromosome III. We have termed the second gene *AtCAP-E2*. The gene products of *AtCAP-E1* and *AtCAP-E2* are 83%

identical to each other and likely arose by genome duplication (Simillion et al., 2002).

AtCAP-E1 complements the yeast *smc2-Δ6* mutant

To confirm that the *AtCAP-E1* gene encodes a functional SMC2 protein, we used it to transform the yeast SMC2 mutant *smc2-Δ6*, which shows a temperature-sensitive defect in chromosome condensation and segregation (Strunnikov et al., 1995). Mutant cells undergo cell-cycle arrest at the non-permissive temperature (37°C). Some of these cells exhibit the classical '*cut*' phenotype wherein the cells have a fully elongated mitotic spindle but their chromosomes fail to separate and appear as a stretched mass of DNA between the two daughter cells. This nuclear morphology is indicative of a defect in chromosome condensation.

We transformed *smc2-Δ6* cells with the *AtCAP-E1* cDNA under the control of the galactose-inducible GAL1 promoter and selected for transformants in the presence of galactose at 37°C. Transformed cells were streaked on plates along with the wild-type and *smc2-Δ6* mutant cells in the presence and absence of galactose and incubated at 37°C. Transformed *smc2-Δ6* cells grew to nearly wild-type levels at 37°C in the presence of galactose (Fig. 1B), but failed to grow in the absence of galactose (Fig. 1C). Fig. 1D-G shows the morphology of the DAPI-stained chromatin by fluorescence microscopy. The stretched nuclear DNA in the *smc2-Δ6* mutant cells and *smc2-Δ6* cells transformed with *AtCAP-E1* cDNA, in the absence of galactose, can be seen in Fig. 1D and E, respectively. Normal chromosome segregation was observed in wild-type cells (Fig. 1F), and transformed cells (Fig. 1G) when grown in the presence of galactose.

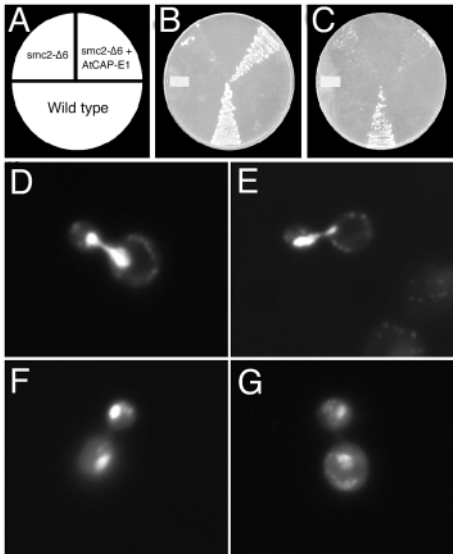

Fig. 1. Functional complementation of the yeast *smc2-Δ6* temperature sensitive mutant with the *AtCAP-E1* cDNA. (A) Diagram of the position on the plates of the cell types in B and C. (B) Rescue of mutant cells transformed with *AtCAP-E1* cDNA in the presence of galactose at 37°C. (C) *smc2-Δ6* mutant cells transformed with *AtCAP-E1* cDNA failed to grow at 37°C in the absence of galactose. (D,E) DAPI-stained mutant and transformed cells, respectively, exhibited the *cut* phenotype in the absence of galactose at 37°C. (F,G) Wild-type and transformed cells, respectively, showed normal chromosome segregation in the presence of galactose at 37°C.

Approximately 500 cells were screened in two independent experiments and the *cut* phenotype was not observed in transformed cells expressing *AtCAP-E1*. To determine the growth profiles of the wild type, mutant and transformed cells, exponentially growing cells were shifted to 37°C and growth curves were established. These experiments demonstrated that the mutant cells transformed with the *AtCAP-E1* construct had growth properties similar to wild-type cells at 37°C (data not shown). Taken together, these results show that *AtCAP-E1* is able to functionally complement the chromosome condensation defect of *smc2-Δ6* cells by rescuing the *cut* phenotype and rendering wild-type levels of growth to mutant cells transformed with the *AtCAP-E1* cDNA. These results support an in vivo role of *AtCAP-E1* in chromosome condensation in *Arabidopsis*.

Differential expression of *AtCAP-E1* and *AtCAP-E2*

The *Arabidopsis* genome contains two SMC2 family members, encoding *AtCAP-E1* and *AtCAP-E2*, which are 90% similar at the protein level. In order to examine the expression profile of both genes, we conducted RT-PCR followed by CAPS analysis (see Materials and Methods). Primers that exactly matched two regions in both genes were used in RT-PCR reactions, and thus the PCR product pool represented transcripts from both genes. The *AtCAP-E1* and *AtCAP-E2* mRNAs were most abundant in roots and young floral buds. The expression was intermediate in stems and low in fully developed leaves and mature siliques (Fig. 2A).

CAPS analysis was employed to assess the relative contribution of the *AtCAP-E1* and *AtCAP-E2* genes to the total SMC2 transcript pool. Based on the sequence of *AtCAP-E1* and the AGI sequence information of *AtCAP-E2*, we digested the PCR products with *Ssp*I or *Xba*I, which represent unique restriction sites in *AtCAP-E1* and *AtCAP-E2* PCR fragments, respectively. Fig. 2B shows that *AtCAP-E1* is expressed at a significantly higher level than *AtCAP-E2* in all tissues tested. The reciprocal CAPS marker restriction enzyme, which cleaves only the *AtCAP-E2* product, gives supporting data (Fig. 2C). Approximately 85% of the transcript pool consisted of *AtCAP-E1* transcripts.

To study the spatial and temporal expression of the *AtCAP-E1* gene, an *AtCAP-E1* promoter::β-glucuronidase (GUS) reporter chimeric gene was constructed and used to generate transgenic plants. Several independent transformants were assayed histochemically for GUS activity, and all primary transformants exhibited the same qualitative expression pattern.

In plants, apical meristems and lateral organ primordia are sites of active cell division. Fig. 2E shows GUS staining of the apex of a young seedling, wherein the entire apical dome and the emerging true leaves are stained. The root apical meristem (RAM) and emerging lateral root primordia also stain intensely (Fig. 2F,G). No activity was observed in differentiated root tissue. In mature plants, strong GUS expression was observed in newly formed organs. Uniform GUS expression was detected during early leaf development, which declined in a basipetal gradient starting from the distal region of immature leaves first (Fig. 2H). The onset of mesophyll cell expansion starts at the leaf tip and progresses towards the leaf base

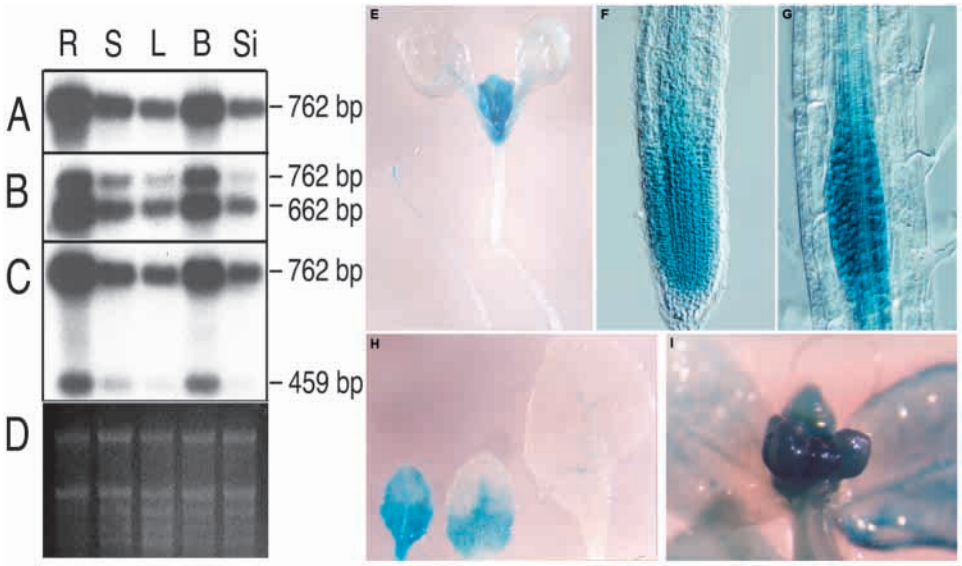

Fig. 2. Expression analysis of *AtCAP-E1* and *AtCAP-E2*. RT-PCR was performed on total RNA from roots (R), stems (S), leaves (L), buds (B), and siliques (Si). (A) DNA gel blot of RT-PCR product pool. (B) PCR products were digested with *Ssp I* (*AtCAP-E1*-specific site) before DNA gel blotting. The intensity of the 662 bp fragment represents the relative abundance of the *AtCAP-E1* transcript. (C) PCR products were digested with *Xba*I (*AtCAP-E2*-specific site) before DNA gel blotting. The intensity of the 459 bp fragment represents the relative abundance of the *AtCAP-E2* transcript. (D) Ethidium bromide-stained gel of 1 μg of total RNA used for reverse transcription showing equal amounts of high quality total RNA. (E-I) *AtCAP-E1* is expressed in meristems and mitotically active tissues. An *AtCAP-E1::GUS* reporter construct was introduced into wild-type *Arabidopsis* plants and GUS activity was examined in the transgenic plants. (E) GUS activity at the apex of an 8-day-old seedling. The apical dome and emerging true leaves stain intensely as does the tip of the root. (F) GUS activity in the primary root apical meristem and in early lateral root primordia (G) emerging from the pericycle cells. (H) GUS activity in developing leaves parallels the basipetal pattern of cell differentiation. (I) intense GUS activity in young floral buds.

forming a gradient of cells at different developmental stages (Pyke et al., 1991). Thus, a decline in GUS activity as development proceeds can be correlated with the decline in mitotic activity. Fig. 2I shows that *AtCAP-E1* is strongly expressed in developing floral buds, which are undergoing active cell division. After organ formation, strong GUS activity was observed in all four floral whorls and staining in young anthers and the gynoecium suggested that the SMC2 gene(s) might be active during meiosis (data not shown). Owing to the long half-life of GUS and the brief duration of meiosis in *Arabidopsis*, it was not possible to be certain if the GUS staining observed in the pollen mother cells (PMCs) was generated during or just prior to meiosis. Therefore, we elected to do RNA in situ hybridization using cross sections of whole inflorescences to precisely define the temporal expression pattern of *AtCAP-E1*. Expression in stamens was observed in the PMCs and in the surrounding tapetal cells during pre-meiotic S phase, prophase I, and anaphase I stages of meiosis (data not shown, but see below).

Identification and characterization of *SMC2* insertion mutants

We undertook a reverse genetics approach to find mutants in the two *Arabidopsis* SMC2 genes. The Arabidopsis Biological Resource Center (ABRC) T-DNA lines were screened to identify insertions into *AtCAP-E1* and we found one pool containing such an insertion. During the course of this work, Liu et al. (Liu et al., 2002) reported that the *titan3* mutant was due to an insertion into this gene, and hence we discontinued characterization of the ABRC line, using the available *ttn3* mutant for additional studies. A T-DNA insertion mutant in the *AtCAP-E2* gene was identified in the Syngenta T-DNA mutant collection (McElver et al., 2001). Sequencing revealed that the insertion occurred at the beginning of the 17th exon. Semi-quantitative RT-PCR revealed no *AtCAP-E2* mRNA in 7-day-old *AtCAP-E2*$^{-/-}$ seedlings (data not shown). To determine the copy number of T-DNA insertions, seeds from the segregating population were grown on BASTA and resistant seedlings were counted (1399 resistant versus 498 sensitive). This ratio closely matched with the expected 3:1 ratio suggesting a single T-DNA insertion. Southern blotting also confirmed that *AtCAP-E2*$^{-/-}$ plants contained a single T-DNA insertion (data not shown).

We could not identify any obvious phenotype associated with the *AtCAP-E2* mutation when the plants were grown under standard conditions.

Double mutants of *AtCAP-E1* and *AtCAP-E2* result in embryo lethality

Since *ttn3* (*AtCAP-E1*$^{-/-}$) plants exhibited a subtle endosperm phenotype with viable embryos and no post-embryonic phenotype, and the *AtCAP-E2*$^{-/-}$ plants demonstrated no obvious defects, we performed genetic crosses between the two homozygous single mutant plants to generate double mutants. The expected relative abundance of each F_2 genotype is given in Table 1. Both mutants are the result of T-DNA insertions: E1 (referring to insertion in *AtCAP-E1*) is marked by an insertion of a kanamycin resistance gene while E2 (referring to insertion in *AtCAP-E2*) contains a BASTA resistance gene. Thus, E1^{-} alleles and E2^{-} alleles would confer resistance to kanamycin and BASTA, respectively (Table 1, column 2). To enrich for double mutants, F_2 seeds were germinated on media containing both antibiotics.

PCR analysis was performed to genotype 180 of the kanamycin and BASTA resistant F_2 plants. If all kanamycin and BASTA resistant genotypes were equally viable, then 1 in 9 of the resistant plants would be expected to have the double mutant genotype (Table 1). However, we did not find any double homozygous mutant plants among the 180 F_2 plants, which is a strong indication that this genotype might be embryo lethal. PCR analysis also revealed another very interesting result. Both the E1$^{+/-}$E2$^{-/-}$ and E1$^{-/-}$E2$^{+/-}$ genotypes were expected to each represent 2/9 of the double antibiotic resistant

Table 1. Characteristics of F_2 progeny of single mutant crosses

Genotype*	Antibiotic resistance†	Relative frequency‡	Observed/expected % ratio of genotypes§
$E1^{+/+}$, $E2^{+/+}$	None	1	–
$E1^{+/+}$, $E2^{+/-}$	BASTA	2	–
$E1^{+/-}$, $E2^{+/+}$	Kanamycin	2	–
$E1^{-/-}$, $E2^{+/+}$	Kanamycin	1	–
$E1^{+/+}$, $E2^{-/-}$	BASTA	1	–
$E1^{+/-}$, $E2^{+/-}$	Kanamycin+BASTA	4	86.66/44.4
$E1^{+/-}$, $E2^{-/-}$	Kanamycin+BASTA	2	13.33/22.2
$E1^{-/-}$, $E2^{+/-}$	Kanamycin+BASTA	2	0.0/22.2
$E1^{-/-}$, $E2^{-/-}$	Kanamycin+BASTA	1	0.0/11.1

*All potential F_2 genotypes of *AtCAP-E1*$^{-/-}$ × *AtCAP-E2*$^{-/-}$ are presented.
†E1 mutants contain a T-DNA conferring kanamycin resistance while E2 mutants contain a T-DNA conferring BASTA resistance.
‡Genotypic frequency relative to the 16 groups in a dihybrid cross.
§Of the F_2 seedlings that germinated on kanamycin+BASTA, the observed/expected ratios of each genotype as confirmed by PCR; *n*=180 plants.

F_2 progeny (Table 1, column 3); thus in 180 plants 40 plants of each genotype would be expected. However, no $E1^{-/-}E2^{+/-}$ plants were observed, and only 24 $E1^{+/-}E2^{-/-}$ plants were recovered. Therefore, analysis of the F_2 population strongly suggests that $E1^{-/-}E2^{-/-}$ and $E1^{-/-}E2^{+/-}$ individuals are genotypes that result in lethality early in development.

The $E1^{-/-}E2^{-/-}$, $E1^{-/-}E2^{+/-}$, and $E1^{+/-}E2^{-/-}$ diploid genotypes all require that at least one of the gametes has the haploid genome $E1^{-}E2^{-}$. Since the three aforementioned genotypes were either missing or under-represented in the F_2 generation, it raised the possibility that the haploid spores with the $E1^{-}E2^{-}$ genotype could not successfully complete gametogenesis. To test this hypothesis we performed reciprocal crosses of wild type with double heterozygotes, $E1^{+/-}E2^{+/-}$, and scored the F_1 seeds for their ability to grow on the kanamycin/BASTA selection media. The types of haploid genotypes that can be produced by the double heterozygote are $E1^{+}E2^{+}$, $E1^{+}E2^{-}$, $E1^{-}E2^{+}$, and $E1^{-}E2^{-}$. Since the wild-type parent only produces the $E1^{+}E2^{+}$ (which is sensitive to both kanamycin and BASTA), only the F_1 offspring that receive the $E1^{-}E2^{-}$ genotype from the double heterozygous parent would be able to grow on the selection medium. Thus only 25% of the F_1 plants would be expected to be resistant to both kanamycin and BASTA. When the $E1^{+/-}E2^{+/-}$ plants were used as the male parent only 3.2% of the F_1 seedlings (*n*=248) were resistant to both antibiotics. Thus, the greatly reduced number of $E1^{+/-}E2^{+/-}$ individuals indicates that only 13% (3.2% observed versus 25% expected) of the expected number of $E1^{-}E2^{-}$ pollen grains are able to successfully complete male gametogenesis. Similarly, in the reciprocal cross in which the $E1^{+/-}E2^{+/-}$ plants were used as the female parent, only 12.5% of the F_1 seedlings (*n*=202) were resistant to both antibiotics. This indicates that there is a 50% reduction in the ability of the megaspore to complete female gametogenesis. Thus, failure during gametogenesis in $E1^{-}E2^{-}$ gametes is a major, but not exclusive source of lethality.

To further investigate the issue of viability we examined the contents of the siliques. An indicator of early lethality in *Arabidopsis* is a paucity of normal seeds in developing siliques. Wild-type and the single mutant plants yielded normal siliques filled with full, green seeds (Fig. 3A-C). However, severe seed defects were observed in the mature siliques of the self-crossed $E1^{+/-}E2^{-/-}$ individuals (Fig. 3D). Among the 26 green siliques that we examined, we observed 43.43% normal green seeds, 30.86% discolored and mis-shapened seeds, and 25.7% unfertilized ovules, which appeared as empty spaces (aborted ovule development presumably associated with failure to complete female gametogenesis) in the silique. We used differential interference contrast microscopy (DIC) to determine the developmental stage at which the embryos in these abnormal seeds were arrested. The normal-appearing green seeds contained normal embryos at the globular to torpedo stages (Fig. 3E). Embryo development clearly differed in the abnormal sibling seeds with embryos arrested at the globular stage of embryogenesis (Fig. 3F). The seeds harboring the mutant embryos were usually smaller. Occasionally, we observed mutant embryos at the late globular stage with

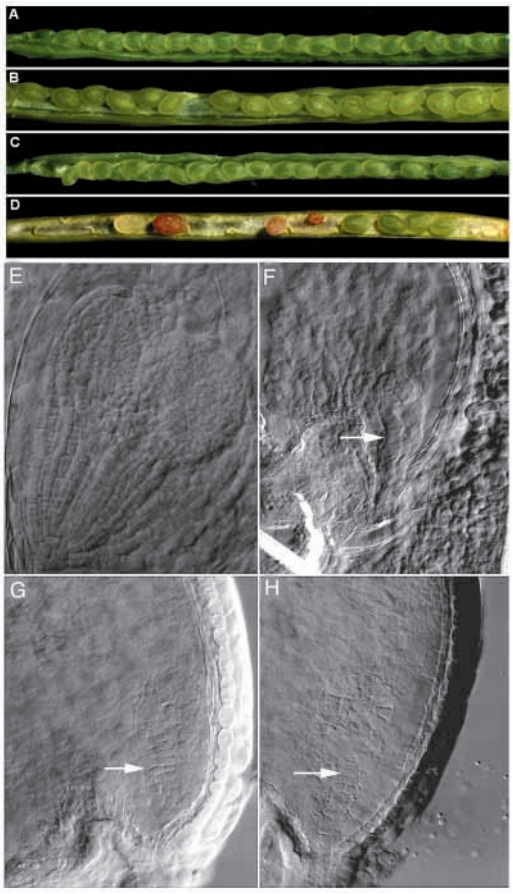

Fig. 3. Seed and embryo defects. (A) Silique from a wild-type Columbia plant with normal green developing seeds filling the entire length of the silique. (B,C) Siliques from (B) an $E1^{-/-}E2^{+/+}$ plant and (C) an $E1^{+/+}E2^{-/-}$ plant with developing seeds similar to those of the wild-type silique. (D) Silique from an $E1^{+/-}E2^{-/-}$ plant with the green seeds containing the normal embryos and brown seeds harboring the aborted embryos. Note the significant number of empty spaces between developing seeds resulting from unfertilized ovules. (E) Differential interference contrast (DIC) microscopy of a normal sibling embryo at the torpedo stage. (F) DIC image of an $E1^{+/-}E2^{-/-}$ embryo arrested at the globular stage. (G,H) DIC images showing patterning defects in the suspensor and embryo proper. Arrows point to suspensors.

distinct defects in cell patterning of the suspensor as well as the embryo proper. The suspensors of these embryos consisted of randomly arranged multi-cell layers with both transverse and longitudinal cell division planes, whereas the suspensors of wild-type embryos consist of single files of six to 11 cells resulting from a series of transverse divisions. Similarly, the abnormal embryos exhibited an altered morphology probably due to atypical cell division planes, resulting in an arrested globular-like embryo (Fig. 3G,H). Thus, our silique analyses show that self-crosses of $E1^{+/-}E2^{-/-}$ individuals often produce many abnormal seeds containing aborted embryos and some seeds fail to form at all.

In our earlier PCR analysis of F_2 progeny of the self-cross of the dihybrid, in addition to not recovering any double homozygous mutants, we also did not recover any plants of the $E1^{-/-}E2^{+/-}$ genotype. To establish that this genotype also is associated with lethality during early development we crossed $E1^{+/-}E2^{-/-}$ (female parent) with $E1^{-/-}E2^{+/+}$ (male parent). In this cross 50% of the progeny are expected to have the $E1^{+/-}E2^{+/-}$ genotype and the other 50% are expected to have the $E1^{-/-}E2^{+/-}$ genotype, but 25% of this latter group are expected to fail because of female gametic inviability (for $E1^{-}E2^{-}$). Thus we expected to find 25% nonviable seeds. We dissected 8 developing siliques from this cross and observed the embryo lethal phenotype in 27.28% of the seeds (n=164). We genotyped 32 progeny seedlings of this cross, and all of the plants were identified as $E1^{+/-}E2^{+/-}$ genotype. Thus, in addition to the double null plants, $E1^{-/-}$ mutants which are heterozygous at the E2 locus, also cannot successfully complete embryogenesis.

Meiotic segregation defects in *AtCAP-E1*$^{+/-}$, *AtCAP-E2*$^{-/-}$ plants

The $E1^{+/-}E2^{-/-}$ genotype was the only genotype we recovered that carries only one functional SMC2 allele. Plants of this genotype often exhibit vegetative abnormalities (see the next section), and we examined meiosis in these plants to assess chromosome condensation/segregation defects. In plants, meiosis punctuates the sporophytic and gametophytic phases of the life cycle. Male meiosis (microsporogenesis) occurs in the pollen mother cells (PMCs) that give rise to four haploid microspores, each of which undergoes mitosis and differentiates into a mature pollen grain. Our GUS reporter gene studies as well as the in situ hybridization experiments indicated that the SMC2 genes are expressed in PMCs, and this fact prompted us to ascertain whether there exists an aberrant chromatin phenotype during meiosis in $E1^{+/-}E2^{+/-}$ and $E1^{+/-}E2^{-/-}$ plants. During meiosis I, chromatin condensation reaches a maximal level at metaphase I/anaphase I and hence we examined PMCs undergoing these two stages during meiosis I. In wild-type PMCs, congression of discrete bivalents was observed, and later, at the onset of anaphase, the chromosomes segregated properly (Fig. 4A,D). Cytological analysis of DAPI-stained PMCs of $E1^{+/-}E2^{+/-}$ plants showed no aberrant chromatin behavior during meiosis I, and normal homologous chromosome segregation was observed (data not shown). In contrast, PMCs of $E1^{+/-}E2^{-/-}$ plants often contained diffuse and non-discrete bivalents at metaphase I (Fig. 4C), and exhibited regions of stretched chromatin bridges during anaphase I with less condensed chromosomes (Fig. 4F). Nonetheless, these chromosomes appeared more condensed than the interphase chromatin as observed by DAPI staining (data not shown). Thus, this meiosis I defect mimics those observed in other condensin mutants during mitosis in yeast (Saka et al., 1994; Strunnikov et al., 1995; Bhalla et al., 2002) and *Drosophila* (Bhat et al., 1996; Steffensen et al., 2001) and during mitosis and meiosis II in *C. elegans* (Hagstrom et al., 2002).

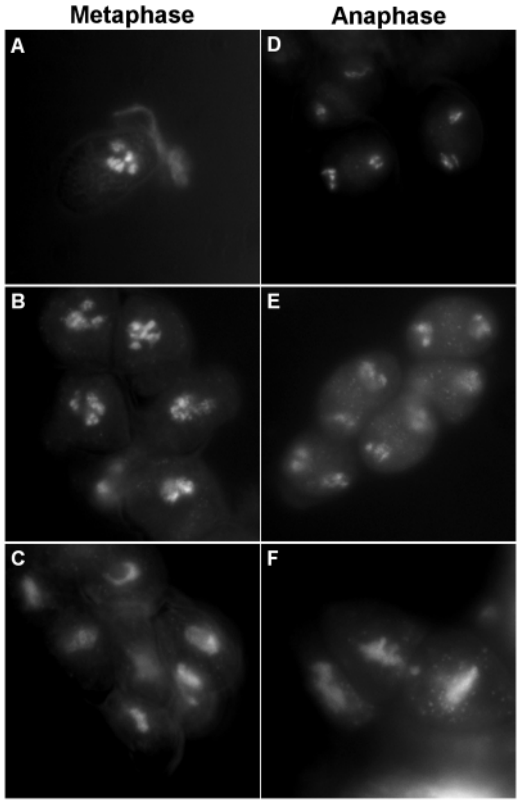

Fig. 4. SMC2 is required for proper meiotic chromosome segregation. Pollen mother cells at both metaphase I and anaphase I from wild-type (A,D) and $E1^{+/-}E2^{-/-}$ plants (B,C,E,F) were stained with DAPI and examined by fluorescence microscopy. In wild type, discrete signals and proper segregation of chromosomes were observed, whereas in a population of the mutant pollen mother cells, either relatively normal (B,E) or diffuse signals and chromatin bridges were often observed (C,F).

Developmental defects of condensin antisense plants

To examine the effects of reduced *AtCAP-E1* and *AtCAP-E2* activity during *Arabidopsis* development, we generated transgenic plants carrying an antisense fragment of the *AtCAP-E1* cDNA under the control of the constitutive CaMV-35S promoter. Ten independent antisense lines were characterized, all of which exhibited varying degrees of similar phenotypic abnormalities. All T1 plants were selfed and seeds of the T_2 generation were selected on kanamycin. Three independent T_2 lines with most severe defects were selected for further analyses.

Although the antisense seedlings germinated with no obvious embryonic defects, pleiotropic phenotypes affecting various stages of post-embryonic development were observed. The transcript levels of both *AtCAP-E1* and *AtCAP-E2* in these

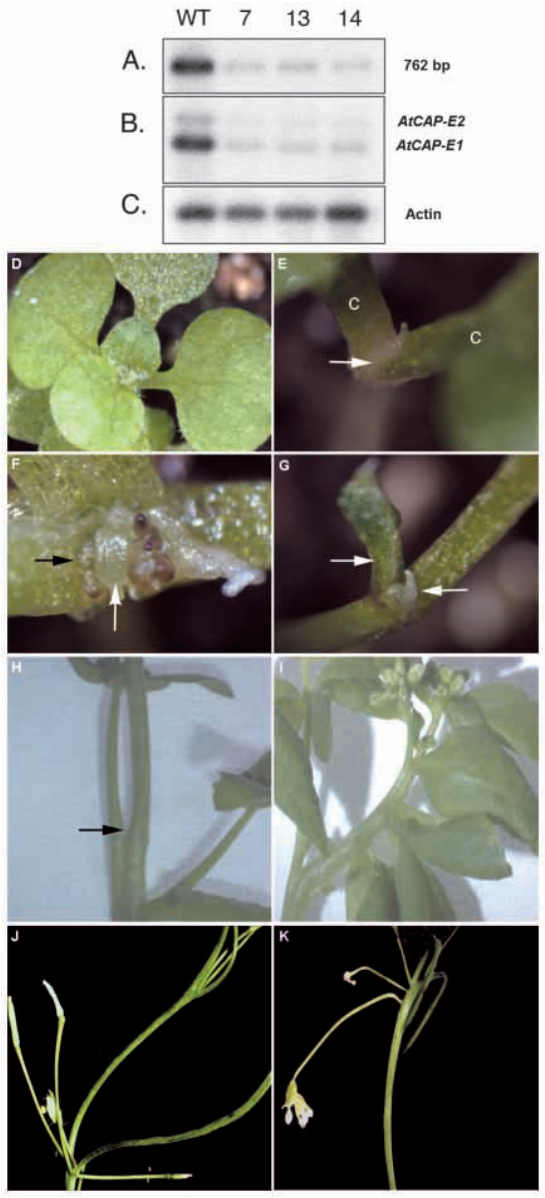

Fig. 5. Reduced *AtCAP-E1* and *AtCAP-E2* levels correlate with developmental defects. (A-C) RT-PCR analysis of SMC2 expression in wild type and three representative antisense lines, 7, 13 and 14. (A,B) RNA was prepared from 7-day-old seedlings and subjected to RT-PCR with the same primers that were used for gene expression RT-PCR. Note that expression is high in wild-type seedlings, but dramatically reduced in the three antisense lines. (B) CAPS analysis (see Fig. 2B and the Methods) of the total RT-PCR pool, illustrating that both genes are affected by the antisense strategy. (C) The same RNA samples used in A and B were subjected to RT-PCR with primers for an actin gene, which served as an internal control for mRNA abundance in each of the samples. (D-K) Developmental defects in the T2 generation of antisense plants. (D) A wild-type *Arabidopsis* seedling at 12 days after germination. (E) A 12-day old antisense seedling exhibiting the severe phenotype where the SAM has failed to initiate any true leaves (c, cotyledons). (F) An 18-day-old antisense plant, illustrating the enlarged and degenerating SAM (white arrow) and an emerging axillary bud (black arrow). (G) Elongated leaf-like structures (arrows) initiated by an enlarged 18-day-old SAM. (H) Stem bifurcation (arrow) associated with fasciation. (I) Altered phyllotaxy of cauline leaves. (J,K) Stem and floral fasciation observed in $E1^{+/-}E2^{-/-}$ plants.

seedlings were dramatically reduced (Fig. 5A-C), confirming a strong antisense suppression of the in vivo *AtCAP-E1* and *AtCAP-E2* transcript pool. In the most severe cases, the shoot apical meristem (SAM) developed into an enlarged dysfunctional mass (Fig. 5E,F) and asymmetric leaf-like structures often formed from the primary SAM (Fig. 5G). However, these plants usually produced axillary buds, which ultimately produced flowering shoots that were developmentally delayed (Fig. 6A,B). Typically, the antisense plants produced shoots with varying degrees of stem and inflorescence fasciation (Fig. 5H/I). Fasciation represents a disruption in the pattern of organogenesis and is associated with breakdown or disruption in SAM structure (Leyser and Furner, 1992), resulting in altered leaf and floral phyllotaxy, and broadening, flattening, and in extreme cases, bifurcation of the stem. Interestingly, stem and floral fasciation was also observed in some $E1^{+/-}E2^{-/-}$ plants (Fig. 5J,K).

DAPI-stained sections of the SAMs of wild-type and antisense plants with the terminal dysfunctional meristem

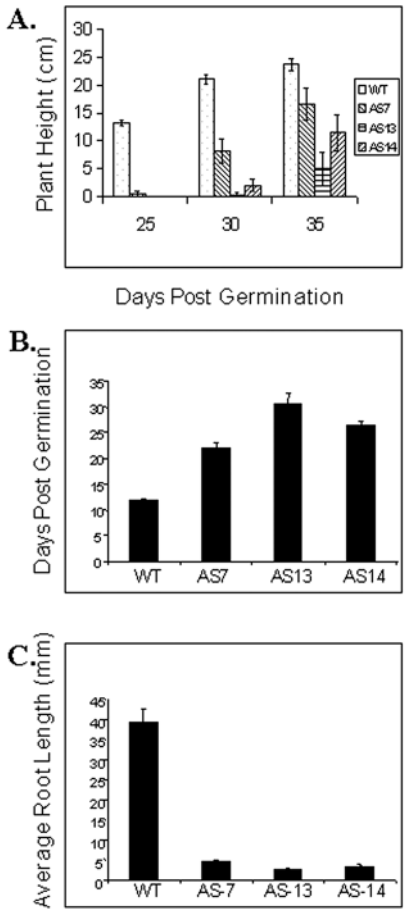

Fig. 6. Plant growth analysis of wild type and three antisense lines. (A) Plant height at 25, 30 and 35 days post germination. Height of the tallest branch was measured for the antisense plants. Standard deviations are indicated for each sample by vertical lines (n=18 per line). (B) Comparison of time (days post-germination) to the floral transition in wild-type and antisense plants (n=18 per line). The emergence of floral buds was detected in individual plants using a dissecting microscope. (C) Comparison of the average root length in 7-day-old vertically grown wild-type and antisense seedlings (n=48 per line).

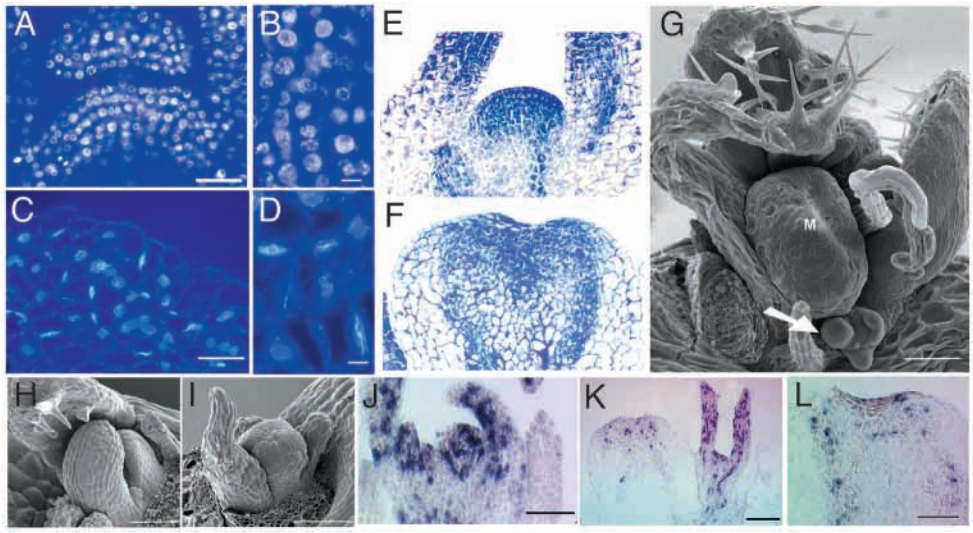

Fig. 7. Cytological and molecular characterization of phenotypic defects in the shoot apical meristems of antisense plants. (A-D) DAPI-stained sections of wild-type (A,B) and antisense (C,D) SAMs. Note the tunica/corpus organization in a wild-type SAM (A) is disrupted in the antisense SAM (C). The apical dome is enlarged and the cells of the antisense SAM are larger. (B,D) Higher magnification of A and C. The chromatin appears partially condensed and stretched. (E,F) Toluidine Blue-stained sections of 8-day-old wild-type (E) and 18-day-old antisense (F) plants. The enlarged SAM in F illustrates large disorganized cells. (G) Scanning electron micrograph of an 18-day-old antisense plant showing the enlarged and irregularly shaped SAM (M). (H,I) SEM of a wild-type (H) and an antisense (I) meristem, illustrating well patterned and regularly shaped cells on an emerging leaf of wild type (H), but a disorganized pattern of irregularly shaped cells in the antisense line (I). Note that the SAM in l H is hidden by the leaf primordia, but has clearly emerged in the antisense plant (I). (J-L) Histone H4 expression in the SAM of a wild-type (J) and an antisense (K) plant as seen by RNA in situ hybridization. (J) High level expression of histone H4 is observed in the wild-type SAM, leaf primordia and developing young leaves. (K) Apex of an antisense plant showing a dramatic reduction in histone H4 expression in the enlarged SAM. (L) Higher magnification photograph of an antisense SAM, illustrating that few cells are histone H4 positive. Bar=50 μm. Scale bars: 50 μm (A,C); 10 μm (B,D); 150 μm (G); 60 μm (H,I); 50 μm (J); 100 μm (K); 50 μm (L).

revealed a clear distinction in nuclear morphology (Fig. 7A-D). In wild-type cells (Fig. 7A,B), uniform and centrally localized nuclear staining typical of interphase nuclei was observed. In contrast, the chromatin of the enlarged meristem of the antisense plants was stretched and localized at the periphery of the cell (Fig. 7C,D). The intensity of DAPI staining in these cells is indicative of partially condensed chromatin, which in addition is displaced to one side of the cell probably by a large vacuole in an irregularly shaped cell (Fig. 7D). The presence of a large vacuole suggests cell differentiation, as the vacuoles of wild-type SAM cells cannot be distinguished by light microscopy. The normal tunica/corpus cellular arrangement of a wild-type SAM into distinctive histological zones consisting of L1, L2 and L3 layers (Fig. 7A,E) was disorganized in the antisense SAMs (Fig. 7C,F). Scanning electron micrographs of the apex revealed an enlarged SAM bearing morphologically altered leaf primordia. Cells of irregular shapes and sizes were observed both in the meristem and in the developing leaf primordia (Fig. 7G-I and data not shown). We used in situ hybridization with an S-phase-specific marker, histone H4, to assess the levels of cell division activity in the SAMs of wild-type and antisense plants. Compared to the high mitotic activity in the wild-type SAMs (Fig. 7J), very few dividing cells were observed in the antisense SAMs (Fig. 7K,L). However, axillary meristems of these plants were relatively normal in appearance (Fig. 7G) and contained an abundance of cycling cells (Fig. 7K).

Morphological abnormalities were also evident in roots of the antisense plants. Root development was delayed with as much as a tenfold reduction in root length 1 week after germination (Fig. 6C). *Arabidopsis* roots can be divided into three zones along the apical-basal axis: the cell differentiation zone, the cell elongation zone, and the meristematic zone (RAM). The cell elongation zone, located just above the RAM, consists of rapidly proliferating and expanding cells with a dense cytoplasm. Cells in this zone are responsible for root growth (Dolan et al., 1993). The cell differentiation zone lies above the elongation zone and consists of fully differentiated cells. Antisense seedlings had a reduced elongation zone, and root hairs emanated from the epidermal cells adjacent to the RAM (Fig. 8A,B). This is in contrast with the wild-type roots where root hairs are elaborated in the differentiation zone. Ten days after germination, antisense roots contained fewer densely cytoplasmic cells in the elongation zone (Fig. 8C,D). The epidermal and cortical cells were enlarged and vacuolated (Fig. 8D,F), a phenotype similar to that observed in the SAM. In addition, the arrangement of the four types of initials in the RAM around the quiescent center was perturbed (Fig. 8E,F).

In summary, partial depletion of AtCAP-E1 and AtCAP-E2 proteins compromises primary meristem structure and function, consistent with a requirement for SMC2 proteins in actively dividing cells during embryonic as well as post-embryonic development.

Dosage effect of SMC2 proteins

We used immunoblotting to assess the SMC2 protein levels in wild type and in different mutant backgrounds, using a polyclonal antiserum raised against a fragment of AtCAP-E1. The antiserum detects a single protein of approximately 130 KDa in a total protein extract from 7-day old wild-type seedlings (Fig. 9, lane1). Based on conceptualized translation, this corresponds well with the size expected for AtCAP-E1 and AtCAP-E2. In antisense seedlings, the signal is reduced dramatically compared to wild type (lanes 2-4). In $E1^{-/-}E2^{+/+}$ plants (*titan 3*), no band was detected confirming that these plants did not contain detectable levels of AtCAP-E1 protein (lane 5). Although AtCAP-E2 should be present in this extract,

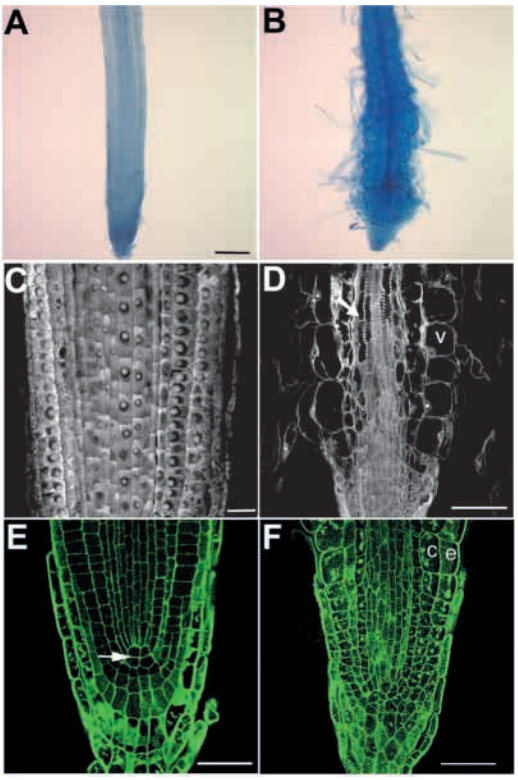

Fig. 8. Phenotypic analysis of 10-day old wild-type and antisense roots. (A,B) Wild-type (A) and antisense (B) roots stained with Aniline Blue. The cell elongation zone of wild-type roots has small, undifferentiated cells with no root hairs. In contrast, antisense roots exhibit disorganized, enlarged, and precociously differentiated cells with root hairs just above the RAM. (C,D) Median optical sections of wild-type (C) and antisense (D) roots stained with propidium iodide showing the cell elongation zone. Note the densely cytoplasmic, small cells with large centrally located nuclei in the wild type (C) compared with the enlarged, vacuolated (v) cells with asymmetrically located nuclei in the epidermal and cortical cell layers in the antisense roots (D). In the antisense root, cell differentiation is also evident from the presence of fully differentiated xylem vessels (D, arrow). (E-F) Median optical sections of wild-type (E) and antisense (F) roots stained with Aniline Blue. Cell organization in wild-type roots is radially symmetric and the quiescent center (arrow in E) is well defined. In antisense roots (F) enlarged epidermal (e) and cortical (c) cells occur in the cell elongation zone, and the quiescent center is disorganized (H). Bars: 250 μm (A,B); 10 μm (C); and 50 μm (D-F).

its levels are too low to be detected by immunoblotting. A faint band was detected from these extracts when six- to eightfold more protein extract was used for immunoblotting (data not shown), suggesting that the sensitivity of immunoblotting is most likely the limiting factor in detecting AtCAP-E2. The protein band detected in the $E1^{+/+}E2^{-/-}$ extract is similar in strength to the wild type (lane 6). Extracts of $E1^{+/-}E2^{-/-}$ plants gave rise to a signal, which was reduced relative to wild type, but significantly more than that of antisense plants (lane 7), pointing to a significant knock-down of both *AtCAP-E1* and *AtCAP-E2* gene products in the antisense plants. Taken together, our data suggest that *Arabidopsis* plants can use both proteins redundantly, that a reduction in SMC2 levels gives

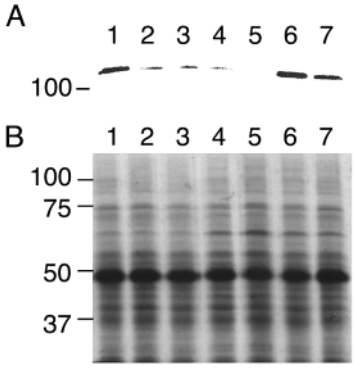

Fig. 9. Immunoblotting of wild type, mutant and antisense lines. (A) Total protein extracts were prepared from 7-day-old seedlings and subjected to immunoblotting. Lane 1: wild-type plant; lanes 2-4, antisense lines; lane 5, $E1^{-/-}E2^{+/+}$ (*titan 3*) plants; lane 6, $E1^{+/+}E2^{-/-}$ plants; lane 7, $E1^{+/-}E2^{-/-}$ plants. (B) Coomassie Blue-stained gel of the protein extracts used in A to show equal loading.

rise to fasciated plants, and that a threshold level of SMC2 molecules is required for normal embryogenesis and development.

DISCUSSION

Expression of SMC2 genes

Our RT-PCR analyses demonstrated that *AtCAP-E1* is expressed at much higher levels than *AtCAP-E2*, but both genes are expressed in a pattern that parallels that of the mitotic activity of the tissues. Meristems and developing tissues of transgenic plants harboring an *AtCAP-E1*::GUS construct stained intensely, whereas more mature tissues showed little or no expression. Similar expression patterns have been observed for other *Arabidopsis* cell cycle genes [*Cdc2a* (Hemerly et al., 1993), *Cyc1At* (Ferreira et al., 1994; Donnelly et al., 1999) and *PROLIFERA* (Springer et al., 2000)] where gene activity was observed only in proliferating tissues. Gene expression of *AtCAP-E1* and *AtCAP-E2* may be regulated by cell cycle-specific factors. Sequence analysis of the promoters of these genes revealed a putative binding site for the E2F transcription factor in each promoter. E2F transcription factors regulate cell cycle-specific gene expression at the G1/S transition (Olivier and Nicholas, 2002). Given our expression data and the presence of putative E2F sites in the promoters, it is likely that these genes are transcriptionally regulated during the cell cycle.

It is also possible that protein activity is controlled by post-translational modifications. In *S. pombe*, the condensin complex is translocated to the nucleus after the phosphorylation of the SMC4 ortholog by the *cdc2* mitotic kinase (Sutani et al., 1999). In *Xenopus* and humans, phosphorylation of a non-SMC component of the complex by *cdc2* has been implicated in supercoiling and condensation activities (Kimura et al., 1998; Kimura et al., 2001), and in *C. elegans*, *AIR-2/AuroraB* kinase-dependent phosphorylation is required for the cell cycle-dependent localization of the condensin complex (Hagstrom et al., 2002). We are currently employing immunocytochemistry to address questions of cell

cycle-dependent expression and localization of SMC2 proteins using synchronized suspension cultured cells.

How do reduced levels of SMC2 influence viability?

In several systems, in vitro experiments have demonstrated that the condensin complex possesses a DNA-dependent ATPase activity that induces positive supercoiling, which probably results in a reorganization of the topology of DNA loop domains (Kimura et al., 1999; Kimura et al., 2001). In *Drosophila*, mitotic defects in embryos and formation of chromatin bridges are caused by mutations in the *BARREN* gene, which encode a non-SMC condensin subunit (Bhat et al., 1996). Similarly, a complete or partial depletion of SMC2/SMC4 transcripts by RNAi treatment in *C. elegans*, results either in embryo lethality or in mature adults with a variety of developmental defects, respectively (Hagstrom et al., 2002). Analysis of the mutant progeny revealed chromosome segregation defects in both somatic and germline cells, and as we observed in *Arabidopsis*, affected cells were abnormally shaped and fecundity was compromised. Thus, in the absence of a functional condensin complex, chromatin may remain relatively decondensed and tangles may remain unresolved, leading to chromosome breakage and abnormal chromosome segregation.

We observed that the highest levels of *Arabidopsis* SMC2 transcripts occur in tissues with high mitotic indices. We were interested in determining if reduced levels of SMC2 protein also affected meiotic chromosome behavior. During meiosis, two distinct nuclear divisions occur to reduce the chromosome number; in the first, homologous chromosomes segregate, while at meiosis II, sister chromatids segregate.

Our GUS and in situ hybridization studies of wild-type plants demonstrated that SMC2 genes are expressed in meiotic cells. But from these studies it was not possible to determine if the SMC2 protein plays a role in the first or second meiotic division, or both. We were not able to recover either $E1^{-/-}E2^{-/-}$ or $E1^{-/-}E2^{+/-}$ mutants due to lethality early in development. However, we did recover a limited number of $E1^{+/-}E2^{-/-}$ plants and examined their chromosome behavior in the first division. These plants showed a reduction in condensation at metaphase and anaphase I, and a mild *cut*-type phenotype at anaphase I. In order for homologous chromosomes to segregate from each other they must resolve the chiasmata, which hold them together. Chiasmata resolution requires that sister chromatids decatenate from each other along the chromosome length. Thus the *cut*-phenotype at meiosis I is probably due to failure to completely decatenate sister chromatids. We did not examine the second meiotic division, but given that the chromosomes did not properly segregate at the first meiotic division, it would be difficult to distinguish affects specific to the second division from secondary effects due to failure at the first division. Our study is the first report demonstrating a role for SMC2 proteins in the first meiotic division. The only other report on the role of SMC2 proteins in meiosis focused on RNAi depletion of the *C. elegans* SMC2 gene [*Mix-1* (Hagstrom et al., 2002)]. These authors reported that depletion of *Mix-1* in meiotic cells did not affect first division segregation, but did affect meiosis II. Compared with our observations, this contrasting result may be due to the fact that the *Mix-1*/*SMC4* condensin complex, unlike the condensin complexes of other organisms, is not associated along the central axis of the chromosome, but instead outlines condensing prophase chromosomes, then localizes specifically to the centromere region.

How do reduced levels of SMC2 affect development?

Development of the aerial parts of plants relies on the activity of meristems, which continuously initiate new organs. Functional meristems are maintained by a coordinated balance between stem cell divisions at the summit of the meristem and loss of cells by differentiation to form primordia at its flanks. The meristem phenotypes we observed could be due to two separate, but not exclusive, mechanisms. First, the morphogenetic consequences could be a direct effect of an altered cell cycle. If chromatin remains relatively decondensed and catenated, the propensity for DNA topological stress is elevated in actively proliferating cells, and this may activate a checkpoint control to result in cell cycle arrest. Indeed, very few cells of the enlarged meristems in antisense plants contain histone H4 mRNA, indicating that most cells have ceased cycling. Other studies involving the perturbation of cell cycle regulatory factors have shown that these also can give rise to meristem defects. *Arabidopsis* plants expressing a dominant-negative form of *cdc2a* can exhibit defects in apical/basal patterning of the embryo, and in some instances meristems elaborate deformed leaves in an incorrect phyllotactic pattern (Hemerly et al., 2000). Similarly, the overexpression of *cyclin D3* results in a variety of developmental defects, including meristem disorganization (Riou-Khamlichi et al., 1999). In root initials, alterations in the activity of a CDK-activating kinase led to differentiation of the initials, followed by cessation of cell division (Umeda et al., 2000).

The second potential mechanism involves epigenetic control of morphogenesis. Evidence is accumulating that condensins and other factors involved in DNA/chromatin dynamics epigenetically alter gene expression programs. One of the regulatory proteins of the *Drosophila* condensin subunit interacts with polycomb group proteins to maintain transcriptional silencing of homeotic genes (Lupo et al., 2001). This indicates that condensin might act in the epigenetic control of gene expression. A similar mechanism has been suggested in the *fasciata* CAF-1 mutant that ectopically expresses the *WUSCHEL* and *SCARECROW* genes (Kaya et al., 2001). Molecular and cytological studies in *Arabidopsis* have included analyses of centromeres and associated heterochromatin, and surprisingly, these regions contain expressed genes, including some encoding putative transcription factors and other signaling molecules (Copenhaver et al., 1999). If the *Arabidopsis* condensin preferentially associates with heterochromatin, it may dictate how and when genes located in heterochromatin are expressed, and in antisense or mutant plants having reduced levels of SMC2, this may lead to misregulation of gene expression. Whether the developmental defects we observed are a direct consequence of chromosomal damage or an indirect effect mediated by an epigenetic mechanism needs to be addressed.

In antisense plants exhibiting severe phenotypes, the primary SAM enlarges into a callus-like mass of tissue and aborts, but functional, albeit fasciated, axillary meristems arise. The difference in sensitivity of the primary and axillary meristems to impaired chromosome condensation in our antisense plants could be due to low expression of the antisense gene from the

35S promoter in axillary meristems or a differential ability of the cells to employ a checkpoint delay in response to defective chromosome segregation. It is possible that the duration of the cell cycle is longer in axillary meristems, which could allow more time for the cells to resolve the chromosomes, allowing them to circumvent damage and proceed through an arrest checkpoint. Although Laufs et al. (Laufs et al., 1998) compared the mitotic indices and cell cycle dynamics in inflorescence and floral meristems in *Arabidopsis* and found them to be similar, to our knowledge no comparative information exists on cell cycle parameters of primary versus axillary meristems.

Threshold levels of SMC2 are required for proper development

Amongst organisms in which SMC2 genes have been characterized, *Arabidopsis* is unique in that it harbors two closely related genes instead of one. Our experiments show that AtCAP-E1 and AtCAP-E2 can act redundantly, as indicated by mild or no defects in the single mutants (compared to the catastrophic consequences of the double null mutant), and the similar expression patterns as gauged by RT-PCR. Although the qualitative patterns of expression are similar, the two genes are differentially expressed, with *AtCAP-E1* transcripts accounting for most of the SMC2 transcript pool. Differential regulation of duplicated genes has been observed in a number of species and probably drives functional divergence (Pickett and Meeks-Wagner, 1995). Such differential regulation might ensure normal development despite physiological or genetic perturbations. It is not known if the duplication of SMC genes in *Arabidopsis* represents a unique situation, or if plants in general have evolved this mechanism to avoid problems associated with improper chromosome condensation.

Although both single mutants are relatively normal, heterozygosity for insertion into one gene in a null background for the second gene confers two distinct phenotypes: lethality during embryogenesis ($E1^{-/-}E2^{+/-}$) or fasciation of relatively normal plants ($E1^{+/-}E2^{-/-}$). This suggests that the effect of the SMC2 proteins is dose dependent. Reducing the AtCAP-E2 level to one half of its level in $E1^{-/-}E2^{+/+}$ plants, which develop normally, results in death during embryogenesis, and suggests that AtCAP-E2, despite its low levels in the cell, has a higher specificity for its target. In the antisense lines, where the expression of both genes is reduced, and in $E1^{+/-}E2^{-/-}$ plants, fasciation occurs, indicating that a critical threshold level of SMC2 proteins are required to sponsor events of chromosome condensation and support normal morphogenesis. The use of SMC2 antibodies in chromatin immunoprecipitation assays may provide some clues on binding specificity and identify target sequences important for condensin complex function.

The authors wish to thank Dr Douglas Koshland for kindly providing the yeast *smc2-Δ6* and wild-type strains, Dr Nicole Chaubet-Gigot for providing the histone H4 clone, and the Arabidopsis Biological Resource Center (Ohio State University) for providing seeds of *titan3*. We also thank Drs Nancy Dengler and Michele Heath for sharing equipment, Sasha Singh and Danielle Vidaurre for assistance with microscopy, David Douda for assistance with genotyping, and Dr Nancy Dengler and Scott Douglas for critical review of the manuscript. We appreciate the helpful advice of three anonymous reviewers. N.U.S. was supported by an Ontario Graduate Scholarship and a University of Toronto Research Fellowship. P.E.S. was supported by a post-graduate fellowship from the Natural Sciences and Engineering Research Council of Canada (NSERC). This research was supported by NSERC research grants to C.A.H. and C.D.R.

REFERENCES

Berger, F. and Gaudin, V. (2003). Chromatin dynamics and *Arabidopsis* development. *Chrom. Res.* **11**, 277-304.

Bhalla, N., Biggins, S. and Murray, A. W. (2002). Mutation in *YCS4*, a budding yeast condensin subunit, affects mitotic and non-mitotic chromosome behavior. *Mol. Biol. Cell* **13**, 632-645.

Bhat, M. A., Philip, A. V., Glover, D. M. and Bellen, H. J. (1996). Chromatid segregation at anaphase requires the *BARREN* product, a novel chromosome-associated protein that interacts with topoisomerase II. *Cell* **87**, 1103-1114.

Clough, J. S. and Bent, A. F. (1998). Floral dip: a simplified method for *Agrobacterium*-mediated transformation of *Arabidopsis thaliana*. *Plant J.* **16**, 735-743.

Copenhaver, G. P., Nickel, K., Kuromori, T., Benito, M., Kaul, S., Lin, X., Bevan, M., Murphy, G., Harris, B., Parnell, L. D., McCombie, W. R., Martienssen, R. A., Marra, M. and Preuss, D. (1999). Genetic definition and sequence analysis of *Arabidopsis* centromeres. *Science* **286**, 2468-2474.

Cuvier, O. and Hirano, T. (2003). A role of topoisomerase II in linking DNA replication to chromosome condensation. *J. Cell Biol.* **160**, 645-655.

Dinardo, S., Voelkel, K. and Sternglanz, R. (1984). DNA topoisomerase II mutant of *Sacchromyces cerevisae*-Topoisomerase II is required for segregation of daughter molecules at the termination of DNA replication. *Proc. Natl. Acad. Sci.* **81**, 2616-2620.

Dolan, L., Janmaat, K., Willemsen, V., Linstead, P., Poethig, S., Roberts, K. and Scheres, B. (1993). Cellular organization of the *Arabidopsis thaliana* root. *Development* **119**, 71-84.

Donnelly, P., Bonetta, D., Taukaya, H., Dengler, R. E. and Dengler, N. G. (1999). Cell cycling and cell enlargement in developing leaves of *Arabidopsis*. *Dev. Biol.* **215**, 407-419.

Ferreira, P., Hemerly, A., Engler, J. A., van Montagu, M., Engler, G. and Inze, D. (1994). Developmental expression of the *Arabidopsis* cyclin gene *cyc1At*. *Plant Cell* **6**, 1763-1774.

Fousteri, M. I. and Lehmann, A. R. (2000). A novel SMC protein complex in *Schizosaccharomyces pombe* contains the Rad18 DNA repair protein. *EMBO J.* **19**, 1691-1702.

Freeman, L., Aragon-Alcaide, L. and Strunnikov, A. (2000). The condensin complex governs chromosome condensation and mitotic transmission of rDNA. *J. Cell Biol.* **149**, 811-824.

Gietz, R. D. and Woods, R. A. (1998). Transformation of yeast by the lithium acetate/single-stranded carrier DNA/PEG method. *Methods Microbiol.* **26**, 53-66.

Gimenez-Abian, J. F., Clarke, D. J., Devlin, J., Gimenez-Abian, M. I., de la Torre, C., Johnson, R. T., Mullinger, A. M. and Downes, C. S. (2000). Premitotic chromosome individualization in mammalian cells depends on topoisomerase II activity. *Chromosoma* **109**, 235-244.

Hagstrom, K. A., Holmes, V. F., Cozzarelli, N. R. and Meyer, B. J. (2002). *C. elegans* condensin promotes mitotic chromosome architecture, centromeric organization, and sister chromatid segregation during mitosis and meiosis. *Genes Dev.* **16**, 729-742.

Hemerly, A., Ferreira, P., Engler, J. A., van Montagu, M., Enlger, G. and Inze, D. (1993). *Cdc2a* expression in *Arabidopsis* is linked with competence for cell division. *Plant Cell* **5**, 1711-1723.

Hemerly, A., Ferreira, P., van Montagu, M., Engler, G. and Inze, D. (2000). Cell division events are essential for embryo patterning and morphogenesis: studies on dominant-negative cdc2aAt mutants of *Arabidopsis*. *Plant J.* **23**, 123-130.

Hirano, T. and Mitchison, T. J. (1994). A heterodimeric coiled-coil protein required for mitotic chromosome condensation *in vitro*. *Cell* **79**, 449-458.

Hirano, T. (2002). The ABCs of SMC proteins: two-armed ATPases for chromosome condensation, cohesion, and repair. *Genes Dev.* **16**, 399-414.

Jackson, D. (1991). In situ hybridization in plants. I: *Molecular Plant Biology: A Practical Approach*, pp. 163-174. Oxford: Oxford University Press.

Jefferson, R. A., Kavanagh, T. A. and Bevan, M. W. (1987). GUS fusions: β-glucuronidase as a sensitive and versatile gene fusion marker in higher plants. *EMBO J.* **6**, 3901-3907.

Jessberger, R. (2002). The many functions of SMC proteins in chromosome dynamics. *Nature Rev. Mol. Cell. Biol.* **3**, 767-778.

Kaya, H., Shibahara, K., Taoka, K., Iwabuchi, M., Stillman, B. and Araki, T. (2001). *FASCIATA* genes for chromatin assembly factor-1 in *Arabidopsis* maintain the cellular organization of apical meristems. *Cell* **104**, 131-142.

Kimura, K., Hirano, M., Kobayashi, R. and Hirano, T. (1998). Phosphorylation and activation of 13S condensin by Cdc2 *in vitro*. *Science* **282**, 487-490.

Kimura, K., Rybenkov, V. V., Crisona, N. J., Hirano, T. and Cozzarelli, N. R. (1999). 13S condensin actively reconfigures DNA by introducing global positive writhe: implications for chromosome condensation. *Cell* **98**, 239-248.

Kimura, K., Cuvier, O. and Hirano, T. (2001). Chromosome condensation by a human condensin complex in *Xenopus* egg extracts. *J. Biol. Chem*. **276**, 5417-5420.

Konieczny, A. and Ausubel, F. M. (1993). A procedure for mapping *Arabidopsis* mutations using codominant ecotype-specific PCR-based markers. *Plant J.* **4**, 403-410.

Laufs, P., Grandjean, O., Jonak, C., Kieu, K. and Traas, J. (1998). Cellular parameters of the shoot apical meristem in *Arabidopsis*. *Plant Cell* **10**, 1375-1389.

Leyser, O. and Furner, I. J. (1992). Characterization of three shoot apical meristem mutants of *Arabidopsis thaliana*. *Development* **116**, 397-403.

Lieb, J. D., Albrecht, M. R., Chuang, P. T. and Meyer, B. J. (1998). *MIX-1*: an essential component of the *C. elegans* mitotic machinery executes X chromosome dosage compensation. *Cell* **92**, 265-277.

Liu, C., McElver, J., Tzafrir, I., Joosen, R., Wittich, P., Patton, D., van Lammeren, A. A. M. and Meinke, D. W. (2002). Condensin and cohesin knockouts in *Arabidopsis* exhibit a *titan* seed phenotype. *Plant J.* **29**, 405-415.

Losada, A., Hirano, M. and Hirano, T. (1998). Identification of *Xenopus* SMC protein complexes required for sister chromaid cohesion. *Genes Dev.* **12**, 1986-1997.

Lupo, R., Breiling, A., Bianchi, M. E. and Orlando, V. (2001). *Drosophila* chromosome condensation proteins topoisomerase II and *barren* colocalize with *polycomb* and maintain Fab-7 PRE silencing. *Mol. Cell* **7**, 127-136.

McElver, J., Tzafrir, I., Aux, G., Rogers, R., Ashby, C., Smith, K., Thomas, C., Schetter, A., Zhou, Q., Cushman, M. A., Tossberg, J., Nickle, T., Levin, J. Z., Law, M., Meinke, D. and Patton, D. (2001). Insertional mutagenesis of genes required for seed development in *Arabidopsis thaliana*. *Genetics* **159**, 1751-1763.

Mengiste, T., Revenkova, E., Bechtold, N. and Paszkowski, J. (1999). An SMC-like protein is required for efficient homologous recombination in *Arabidopsis*. *EMBO J.* **18**, 4505-4512.

Michaelis, C., Ciosk, R. and Nasmyth, K. (1997). Cohesins: Chromosomal proteins that prevent premature separation of sister chromatids. *Cell* **91**, 35-45.

Muller, C. and Leutz, A. (2001). Chromatin remodeling in development and differentiation. *Curr. Opin. Genet. Dev.* **11**, 167-174.

Olivier, S. and Nicholas, J. D. (2002). A revised picture of the E2F transcriptional network and RB function. *Curr. Opin. Cell Biol.* **14**, 684-691.

Pickett, F. B. and Meeks-Wagner, D. R. (1995). Seeing double: appreciating genetic redundancy. *Plant Cell* **7**, 1347-1356.

Pyke, K. A., Marrison, J. L. and Leech, R. M. (1991). Temporal and spatial development of the cells of the expanding first leaf of *Arabidopsis thaliana* (L.) Heynh. *J. Exp. Bot.* **42**, 1407-1416.

Reyes, J. C., Hennig, L. and Gruissem, W. (2002). Chromatin remodeling and memory factors. New regulators of plant development. *Plant Physiol.* **130**, 1090-1101.

Riha, K., McKnight, T. D., Griffing, L. R. and Shippen, D. E. (2001). Living with genome instability: Plant responses to telomere dysfunction. *Science* **291**, 1797-1800.

Riou-Khamlichi, C., Huntley, R., Jacqmard, A. and Murray, J. A. H. (1999). Cytokinin activation of *Arabidopsis* cell division through a D-type cyclin. *Science* **283**, 1541-1544.

Saka, Y., Sutani, T., Yamashita, Y., Saitoh, S., Takeuchi, M., Nakaseko, Y. and Yanagida, M. (1994). Fission yeast *cut3* and *cut14*, members of a ubiquitous protein family, are required for chromosome condensation and segregation in mitosis. *EMBO J.* **13**, 4938-4952.

Simillion, C., Vandepoele, K., van Montagu, M. C. E., Zabeau, M. and van de Peer, Y. (2002). The hidden duplication past of *Arabidopsis thaliana*. *Proc. Natl. Acad. Sci. USA* **99**, 13627-13632.

Springer, P. S., Holding, D. R., Groover, A., Yordan, C. and Martiensen, R. A. (2000). The essential Mcm7 protein PROLIFERA is localized to the nucleus of dividing cells during the G1 phase and is required maternally for early *Arabidopsis* development. *Development* **127**, 1815-1822.

Steffensen, S., Coelho, P. A., Cobbe, N., Vass, S., Costa, M., Hassan, B., Prokopenko, S. N., Bellen, H., Heck, M. M. S. and Sunkel, C. E. (2001). A role for *Drosophila* SMC4 in the resolution of sister chromatids in mitosis. *Curr. Biol*. **11**, 295-307.

Strunnikov, A. V., Hogan, E. and Koshland, D. (1995). SMC2, a *Saccharomyces cerevisiae* gene essential for chromosome segregation and condensation, defines a subgroup within the SMC family. *Genes Dev*. **9**, 587-599.

Sutani, T., Yuasa, T., Tomonaga, T., Dohmae, N., Takio, K. and Yanagida, M. (1999). Fission yeast condensin complex: Essential roles of non-SMC subunits for condensation and Cdc2 phosphorylation of Cut3/SMC4. *Genes Dev*. **13**, 2271-2283.

Takahashi, T., Matsuhara, S., Abe, M. and Komeda, Y. (2002). Disruption of a DNA topoisomerase I gene affects morphogenesis in *Arabidopsis*. *Plant Cell* **14**, 2085-2093.

Tian, L. and Chen, Z. J. (2001). Blocking histone deacetylation in *Arabidopsis* induces pleiotropic effects on plant gene regulation and development. *Proc. Natl. Acad. Sci. USA* **98**, 200-205.

Umeda, M., Umeda-Hara, C. and Uchimiya, H. (2000). A cyclin-dependent kinase-activating kinase regulates differentiation of root initial cells in *Arabidopsis*. *Proc. Natl. Acad. Sci. USA* **97**, 13396-13400.

Wagner, D. (2003). Chromatin regulation of plant development. *Curr. Opin. Plant Biol.* **6**, 20-28.